December, 1983] © 1983 The Chemical Society of Japan Bull. Chem. Soc. Jpn., 56, 3827—3829 (1983) 3827

Studies on Salt Hydrates for Latent Heat Storage. IV. Crystallization in the Binary System CH_3CO_2Na-H_2O

Takahiro WADA,* Fumiko KIMURA, and Yoshihiro MATSUO
Central Research Laboratory Matsushita Electric Industrial Co. Ltd., 1006 Kadoma, Osaka, 571

(Received February 21, 1983)

In the binary system CH_3CO_2Na–H_2O, crystallization temperature on slow cooling from a melt, glass transition temperature and crystallization temperature on slow heating from a quenched vitrified solid were measured by varying the CH_3CO_2Na concentration. The crystallization behaviour in the binary system CH_3CO_2Na–H_2O is characterized as follows; (1) crystallization region of ice extends into the CH_3CO_2Na-rich side from the eutectic composition, (2) a hard crystallization region exists in the composition between CH_3CO_2Na 35wt% and 40wt%, (3) the crystallization temperature range of $CH_3CO_2Na\cdot 3H_2O$ is from −50 °C to −30 °C and very narrow.

Sodium acetate trihydrate ($CH_3CO_2Na\cdot 3H_2O$) has recently attracted attention as a useful heat stroage material because of its large latent heat of fusion (about 264 J/g).[1,2] The $CH_3CO_2Na\cdot 3H_2O$ melt tends to supercool even when it is cooled considerably below its melting point (58.4 °C).[3,4] Such a supercooling phenomenon impaired its practical application.[5] Therefore, in order to develop latent heat storage materials using salt hydrates such as $CH_3CO_2Na\cdot 3H_2O$, Kimura[6] studied the supercooling phenomena of some salt hydrates from the viewpoint of the chemical potential difference of water molecules in molten and crystalline states. Wada and Yamamoto[7] have searched for crystal nucleation catalysts of $CH_3CO_2Na\cdot 3H_2O$ and found $Na_4P_2O_7\cdot 10H_2O$.

The phase diagram of the binary system CH_3CO_2Na–H_2O based on data from Seidell's compilation[8] is shown in Fig. 1. A dashed line in Fig. 1 is the liquidus line of metastable CH_3CO_2Na. It is clear from the phase diagram that H_2O and $CH_3CO_2Na\cdot 3H_2O$ form an eutectic mixture melting at −18 °C, with the composition of 23 wt% CH_3CO_2Na and 77 wt% H_2O.

This paper reports a quantitative investigation of the crystallization behavior of the binary system CH_3CO_2-Na-H_2O, where crystallization temperature on slow cooling from a melt (t_c), glass transition temperature (T_g), and crystallization temperature on slow heating from a quenched vitrified solid (T_c) were measured by varying the CH_3CO_2Na concentration.

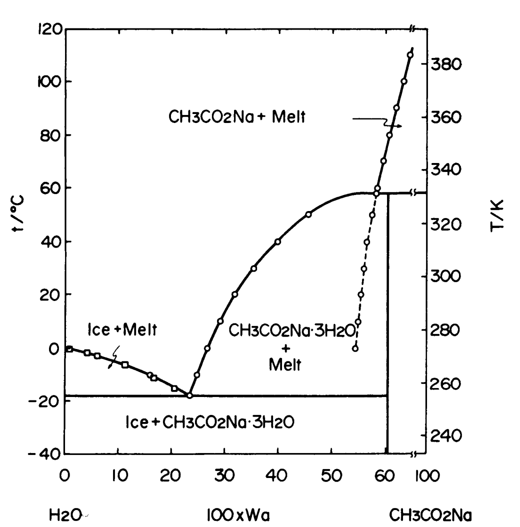

Fig. 1. Phase diagram of the binary system CH_3CO_2Na–H_2O.
○: The data obtained by Green,[9] □: the data obtained by Sidgwick and Gentle.[10]

Experimental

Sodium acetate trihydrate was of a guaranteed grade reagent from Wako Pure Chemical Industry. Weighed quantities of $CH_3CO_2Na\cdot 3H_2O$ and distilled water, 30 g in total, were placed in a glass vessel with a stirring bar. The sample temperature was measured by a chromel–alumel thermocouple attached to the inner wall of the glass vessel which was sealed and immersed in a water bath. In order to obtain reproducible data, the sample was heated to a temperature which is about 10 °C higher than its liquidus temperature and was stirred to a homogeneous melt.[11] Then, the melt was cooled at the rate of about 5 °C/min by consecutive addition of ice to the water bath. When the temperature of the melt reached to 20 °C, the vessel was transferred from the water bath to an ethanol bath. Cooling was continued to −70 °C at the rate of about 5 °C/min by consecutive addition of solid carbon dioxide to the ethanol bath. In such a slow cooling process, crystallization of the sample was detected by a sudden rise in temperature of the melt and by visual inspection. The viscosity of melts increased on cooling, which contained CH_3CO_2Na more than $W_a=0.35$ (W_a is the mass fraction of CH_3CO_2Na), and sometimes the magnetic stirrer failed to operate the stirring bar. The measurement was performed three times for each sample. In this manner, t_c was measured as a function of the CH_3CO_2Na concentration. Figure 2 shows the average and the range of crystallization temperatures obtained by the present measurements.

Temperatures, T_g and T_c were measured as a function of the CH_3CO_2Na concentration by the differential scanning calorimetry (DSC). The DSC measurement was performed by using an SSC 560S DSC (Daini Seikosha Co.), heat-flux DSC. One drop of a melt (about 10 mg) was placed in a 15 μl silver crucible. This crucible was sealed and immersed in a water bath, whose temperature was about 10 °C higher than a liquidus temperature of the sample. After thirty minutes, the crucible was transferred into liquid nitrogen. The overall cooling rate was about 1000 K/min. DSC measurements were performed at a heating rate of 5 °C/min from −130 °C to 70 °C. This DSC system was calibrated by using ice (mp: 0.0 °C), chloroform (mp: −63.5 °C), acetone (mp: −94.3 °C), and ethanol (mp: −114.2 °C) as standards, and the measurements were made two times for each sample.

Results and Discussion

Crystallization Temperature on Slow Cooling from a Melt

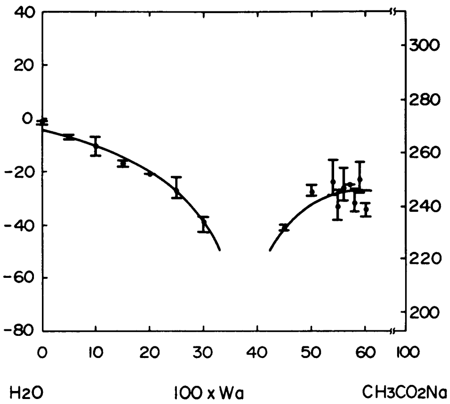

Fig. 2. Crystallization temperature on slow cooling (t_c) in relation to the CH_3CO_2Na concentration.

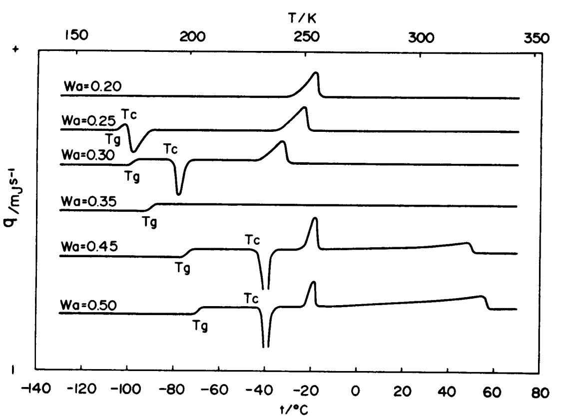

Fig. 3. DSC curves for some quenched samples of the system CH_3CO_2Na–H_2O.

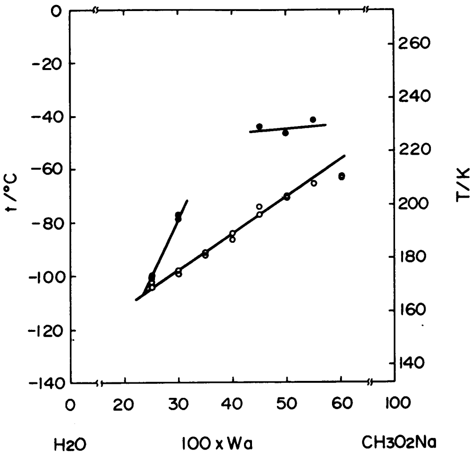

Fig. 4. Glass transition temperature (T_g) and crystallization temperature on slow heating (T_c) in relation to the CH_3CO_2Na concentration.
○: T_g, ●: T_c.

(t_c). The t_cs obtained are shown in Fig. 2. The number on the abscissa, $100 \times W_a$, is the weight percentage of CH_3CO_2Na in the system. The samples of $W_a = 0.35$ and $W_a = 0.40$ did not crystallize in all the runs.

In the water-rich side of the eutectic composition, the t_c curve lies about 5 °C lower than the liquidus line of H_2O, ice crystallizing first from the melt. Interestingly, the t_c curve extends beyond the eutectic composition into the CH_3CO_2Na-rich side. Therefore, the crystals that separated out first from the melt in the CH_3CO_2Na-rich side of the eutectic composition ($W_a = 0.30$) is not $CH_3CO_2Na \cdot 3H_2O$, but ice.

From Fig. 2, it is also clear that t_cs of the melts containing CH_3CO_2Na more than $W_a = 0.45$ are about 90 °C lower than the liquidus line, *i.e.*, supercooling of these samples is about 90 °C. $CH_3CO_2Na \cdot 3H_2O$ separated out first from both melts of $W_a = 0.45$ and $W_a = 0.50$, but for the samples containing CH_3CO_2Na more than $W_a = 0.54$, anhydrous CH_3CO_2Na crystals separated out from their melts at the temperature about 10 °C lower than their liquidus temperarures, followed by crystallization of $CH_3CO_2Na \cdot 3H_2O$. Anhydrous CH_3CO_2Na crystals were identified by X-ray diffraction. Since the t_c curve varies continuously with the CH_3CO_2Na concentration between $W_a \times 0.45$ and $W_a = 0.603$ ($CH_3CO_2Na \cdot 3H_2O$), the curve in Fig. 2 also suggests that anhydrous CH_3CO_2Na crystals (separated out first) have little influence on the subsequent crystallization of $CH_3CO_2Na \cdot 3H_2O$.

Glass Transition Temperature (T_g) DSC curves for some quenched samples are illustrated in Fig. 3, where q is heat flux. T_g and T_c are plotted against the CH_3CO_2Na concentration in Fig. 4. The melt with $W_a = 0.25$ vitrified by quenching, but that with $W_a = 0.20$ did not, and this result was confirmed by visual observation of these samples in a 3 mm diameter pyrex glass tubes put into liquid nitrogen. This observation shows that the glass forming composition is limited on the CH_3CO_2Na-rich side from the eutectic composition ($W_a = 0.23$). This is due to the difficulty of crystal nucleation of $CH_3CO_2Na \cdot 3H_2O$.

In Fig. 4, T_g varies linearly with the CH_3CO_2Na concentration, and those of the samples containing CH_3CO_2Na more than $W_a = 0.55$ lie below the T_g line. This deviation results from the decrease of the CH_3CO_2Na concentration caused by separation of CH_3CO_2Na crystals from the quenched samples, which is confirmed by visual observation using thin glass tubes. Williams and Angell,[12] and Kanno *et al.*[13] have reported that T_g of the sample with $W_a = 0.313$ ($CH_3CO_2Na \cdot 10H_2O$) is −99 and −102 °C, respectively. The T_g estimated from our data is −96 °C and in good agreement with the reported data. The extrapolation of the obtained T_g to pure water gives −140 °C as the T_g of glassy water. Angell and Sare[14] also gave a similar value (−138 °C) from the studies on a large number of aqueous electrolyte solutions. This value is almost identical with the glass transition temperature (−139 °C) obtained for amorphous solid water prepared by the vapor deposition method.[15] The extrapolation to pure $CH_3CO_2Na \cdot 3H_2O$ gives −56 °C as the T_g of glassy $CH_3CO_2Na \cdot 3H_2O$. This value is close to T_g of $Na_2S_2O_3 \cdot 5H_2O$ ($T_g = -42$ °C)[16] and $Ca(NO_3)_2 \cdot 4H_2O$ ($T_g = -54$ °C).[14]

Crystallization Temperature on Slow Heating from a Quenched Sample (T_g) The quenched samples with $W_a = 0.25$ and $W_a = 0.30$ always crystallize on heating after the glass transition. T_c of the sample with $W_a = 0.313$ ($CH_3CO_2Na \cdot 10H_2O$) has been reported to be −73 °C by Kanno *et al.*,[12] which is in good agreement with T_c estimated from our data, −72 °C. The DSC curves show that the melting points of the samples with W_a=0.25 and W_a=0.30 are at −22 and −31 °C, respectively. These melting points are lower than the eutectic point, −18 °C, and lie on the extrapolated liquidus line of H_2O. As shown in Fig. 3, the samples with W_a=0.25 and W_a=0.30 do not show the endothermic peak of $CH_3CO_2Na \cdot 3H_2O$ melting. Therefore, ice is the only compound crystallized from the melts with W_a=0.25 and W_a=0.30. This result is similar to the crystallization behaviour observed on slow cooling of the melt.

The quenched samples with W_a=0.35 and W_a=0.40 did not crystallize on heating twice. As mentioned above, these samples did not crystallize on cooling either. These results show that these samples have a stable solution structure with hard crystallization.

The quenched samples with W_a=0.45, W_a=0.50, and W_a=0.55 crystallized only once in two runs. For these cases, T_cs are between −40 and −50 °C as shown in Fig. 4. $CH_3CO_2Na \cdot 3H_2O$ (W_a=0.603) did not crystallize on heating in two runs.

The phase diagram of the binary system CH_3CO_2Na–H_2O(Fig. 1), t_c cuves (Fig. 2), and T_g line and T_c curves (Fig. 4) are summarized in Fig. 5. In the temperature region demarcated by t_c and T_c curves, ice or CH_3CO_2-$Na \cdot 3H_2O$ is considered to crystallize from the melt in the present experimental conditions. The crystallization behavior of the binary system CH_3CO_2Na–H_2O is characterized as follows: (1) the crystallization region of ice extends into the CH_3CO_2Na-rich side from the eutectic composition, (2) a hard crystallization region exists in the composition between W_a=0.35 and W_a=0.40, (3) the crystallization temperature range of CH_3-$CO_2Na \cdot 3H_2O$ is from −50 °C to −30 °C and very, narrow.

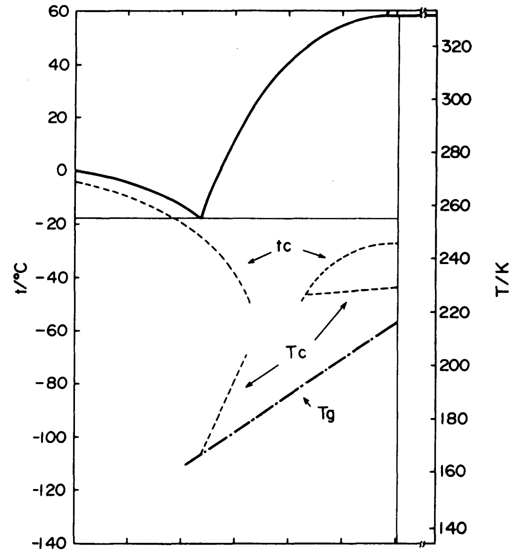

Fig. 5. Crystallization temperature curves (t_c and T_c curves), and glass transition temperature line shown in the phase diagram of the binary system CH_3CO_2Na–H_2O.

The crystallization temperature is generally influenced by the heating or cooling rate, quantity and purity of the sample and stirring method, *etc.* In measuring t_c, if the cooling rate is slower than 5 °C/min or the sample quantity is larger than 30 g, t_cs will be higher than the obtained values. In measuring T_c, if the heating rate is slower than 5 °C/min or the sample quantity is larger than about 10 mg, T_cs will be lower than the obtained values. Therefore, crystallization temperature breadths of ice and $CH_3CO_2Na \cdot 3H_2O$ are expected to be wider than those shown in Fig. 5.

The authors wish to express their thanks to Dr.Ryoichi Kiriyama for his useful discussions and Drs. Tsuneharu Nitta, Eiichi Hirota, and Masanari Mikoda for their continuous encouragements. The authors are grateful to Dr. Ryoichi Yamamoto for his discussions throughout this work.

References

1) M. Telkes, "Solar Materials Science," ed by L. E. Murr, Academic Press, New York (1980), Chap. 11.
2) A. Pebler, *Thermochim. Acta*, **13**, 109 (1975).
3) F. de Winter, *Solar Energy*, **17**, 379 (1975).
4) K. Narita and J. Kai, *J. Int. Electr. Eng. Jpn.*, **101**, 15 (1981).
5) M. Telkes, *Ind. Eng. Chem.*, **44**, 1308 (1952).
6) H. Kimura, *J. Jpn. Assoc. Cryst. Growth*, **7**, 215 (1980).
7) T. Wada and R. Yamamoto, *Bull. Chem. Soc. Jpn.*, **55**, 3603 (1982).
8) A. Seidell, "Solubility of Inorganic and Metal-Organic Compounds," 4th ed, ed by the American Chemical Society, Washington D. C. (1965), Vol. II, p. 854.
9) W. F. Green, *J. Phys. Chem.* **12**, 655 (1908).
10) N.V. Sidgwick and J. A. Gentle, *J. Chem. Soc.*, **121**, 1837 (1922).
11) R. Kiriyama and K. Yamada, *Nippon Kagaku Zasshi*, **71**, 558 (1950).
12) E. Williams and C. A. Angell, *J. Phys. Chem.*, **81**, 232 (1977).
13) H. Kanno, I. Shirotani, and S. Minomura, *Bull. Chem. Soc. Jpn.*, **54**, 2607 (1981).
14) C. A. Angell and E. J. Sare, *J. Chem. Phys.* **52**, 1058 (1970).
15) M. Sugisaki, H. Suga, and S. Seki, *Bull. Chem. Soc. Jpn.*, **41**, 2591 (1968).
16) S. Seki, "Structural Chemistry in Solid," ed by I. Nitta *et al.*, Kagaku Dojin, Kyoto (1968), Chap. 3.